The cosmic ray flux observed at zenith angles larger than 60 degrees with the Pierre Auger Observatory

R.A. Vázquez * for the Pierre Auger Collaboration
*University of Santiago de Compostela, Campus Sur s/n, 15782 Santiago de Compostela, Spain
vazquez@fpaxp1.usc.es

Abstract. **The cosmic ray energy spectrum is obtained using inclined events detected with the surface detectors of the Pierre Auger Observatory. Air showers with zenith angles between 60 and 80 degrees add about 30% to the exposure. Events are identified from background based on compatibility between the arrival time and the detector location enabling the elimination of random signals. The arrival direction is computed using the time information. The core position and a shower size parameter are obtained for each event by fitting measured signals to those obtained from predictions of two-dimensional distributions of the patterns of the muon densities at ground level. The shower size parameter, a zenith angle independent energy estimator, is calibrated using the shower energy measured by the fluorescence technique in a sub-sample of high-quality hybrid events. The measured flux is in agreement with that measured using showers of zenith less than 60 degrees.**

I. INTRODUCTION

Inclined showers are routinely detected by the Pierre Auger Observatory. The Surface Detector (SD) uses 1.2 m deep water–Cherenkov detectors that are sensitive to inclined muons. Hybrid events, events detected simultaneously by the SD and the Fluorescence Detector (FD), provide a method to cross calibrate the Surface Detector even for inclined events.

The analysis of inclined showers is important. It increases the aperture by about 30 % relative to showers with zenith angle less than 60° as used in [12], [10] and has access to regions of the sky which are not visible in the vertical. In addition, inclined showers created by nuclear primaries constitute the background for neutrino detection [5], [15]. Moreover, the inclined showers are characterised by being composed mainly of muons. Therefore they give additional information on the high energy processes in the shower, relevant to the study of composition and of hadronic processes at high energy, see also [16].

Due to the increasing slant depth with the zenith angle, the electromagnetic component is rapidly absorbed as the zenith angle increases. Above $60°$, showers still contain a significant electromagnetic component. For zenith angles larger than 70° the electromagnetic shower is absorbed in the atmosphere and only an electromagnetic 'halo' due to muon decay and other muonic processes survive and account for $\sim 15\%$ of the signal. Due to the long paths traversed, the muons can be deflected by the magnetic field and produce complex patterns at ground where the cylindrical symmetry is lost, depending on the angle between the arrival direction of the shower and the magnetic field. For highly inclined showers ($\geq 80°$), the magnetic deflection can be so large as to separate the positive and negative muons. This makes the use of the one dimensional lateral distribution functions (LDF), used for zenith angles $< 60°$, unsuitable for analysis of inclined showers. Monte Carlo simulations are used to produce maps of muons arriving at ground. These are either parameterised or kept as histogrammed maps and are used to reconstruct the shower core and a shower size parameter. The electromagnetic component is also parameterised independently using Monte Carlo simulations. Inclined events are reconstructed in a similar manner to the vertical events but taking into account the specific characteristics of inclined showers.

Here we present an update of the analysis of inclined events, in the range from 60° to 80°, in the Pierre Auger Observatory for energies above 6.3 EeV, see also [3], [4].

II. EVENT SELECTION

Events are selected using a chain of quality cuts and triggers, which are similar to the trigger chain used in vertical events [6]. After the single detector triggers, the T3 trigger is the lowest array trigger criterion. Data acquisition distinguishes two types: compact triangles of detectors with long signals and preset patterns of detectors with any signal exceeding a certain threshold. For inclined showers, given their elongated patterns, the more important one is the second, being 63 % of all the events in the 60°–80° zenith angle range. For showers between 70°–80° this fraction increases to 87%.

T3 recorded events are selected at the next trigger level (T4), the physical trigger, if they fulfil a time compatibility test. It is based on a "top down" algorithm where, selected stations are iteratively required to have small time residuals compared to a shower front. In addition a criteria of compactness is also applied. The algorithm is used to iterate over the accepted number of stations until a compatible configuration is obtained.

T4 candidates are reconstructed and their arrival direction, shower size, and the core position are determined. The procedure is described in the next section. For the spectrum analysis high quality events are selected at the next trigger level, the T5 [7], the criteria being that the core must be reconstructed accurately to guarantee

a good energy estimation by avoiding events close to the border of the array or events which fall in an area where stations are inactive. Several alternatives were considered. The one currently used (T5HAS) consists of accepting only events were the station closest to the reconstructed core is surrounded by a hexagon of active stations.

The acceptance of the array is then computed geometrically, counting the number of active hexagons, and the aperture is calculated for each array configuration as a function of time. Events with zenith angle greater than 80° are not considered in this analysis, as the uncertainty in the angular reconstruction increases with zenith angle, growing rapidly above 80°. Also at larger zenith angles, due to the low density of muons, the fluctuations are larger and the energy reconstruction has large uncertainty. The total accumulated exposure from 1 January 2004 to 31 December 2008 for zenith angles $< 60^\circ$ is 12790 km^2 sr year, the exposure for zenith angles between 60° and 80° corresponds to 29 % of that value. Over 80000 events were found which pass the T5HAS criteria in the period considered.

III. Angular and Shower Size Determination

The angular and energy determination of inclined events follows a similar pattern to that for vertical events. For the angular reconstruction the start times of the stations are corrected, taking into account the altitude of the station and the curvature of the Earth (due to the elongated shapes, the shower can spawn several tens of kilometers). The corrected start times are checked against the shower front and the arrival direction is obtained by χ^2 minimisation. We have tested several approaches to the angular reconstruction. In addition, good quality hybrid events can be compared with the Fluorescence Detector reconstruction. Overall, the angular resolution is of the order of 1° [8].

For the energy reconstruction the measured signals are compared to the expected ones using the following procedure. First the expected electromagnetic signal, parameterised with Monte Carlo simulations[9], is subtracted from the total signal. At zenith angles $\gtrsim 60^\circ$ the electromagnetic contribution is still appreciable and forms significant fraction of the signal. At larger zenith angles $\gtrsim 70^\circ$, the electromagnetic contribution from π^0 decay is negligible and only a contribution from the decay of the muons themselves (and other processes) is present. This constitute a fraction of the order of 15 %. After the electromagnetic component has been subtracted, the muonic signal is compared to the expected one taken from 'muon maps'. For inclined events, the lack of cylindrical symmetry around the shower axis makes the use of a single variable LDF impossible. Instead, we have developed muon maps which parameterise the muon number expected as a function of the zenith and azimuth angle. This parameterisation of the muon maps is done in the plane perpendicular to the shower arrival direction. In addition, the response of the detector to inclined muons has been calculated using GEANT4. In the figure 1, we show the probability of muons to produce a given signal for several zenith angles and muon energies. A single muon arriving at 80° zenith angle can produce a signal of more than 3 VEM.

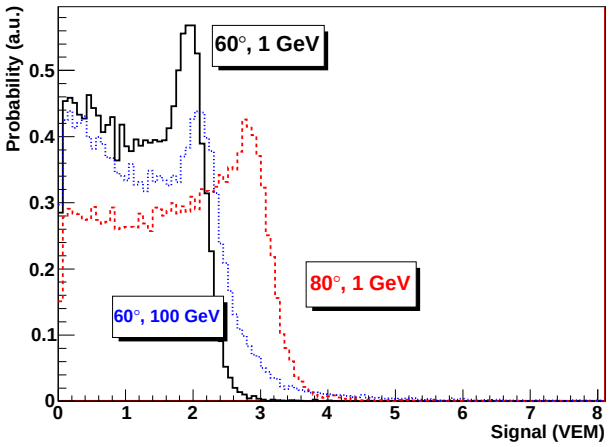

Fig. 1. Surface detector response to inclined muons. Probability of measuring a signal in VEM (vertical equivalent muon) for muons of zenith angle 60° and energy 1 GeV (continuous histogram), 60° and 100 GeV (dotted histogram), and 80° and 1 GeV (dashed histogram).

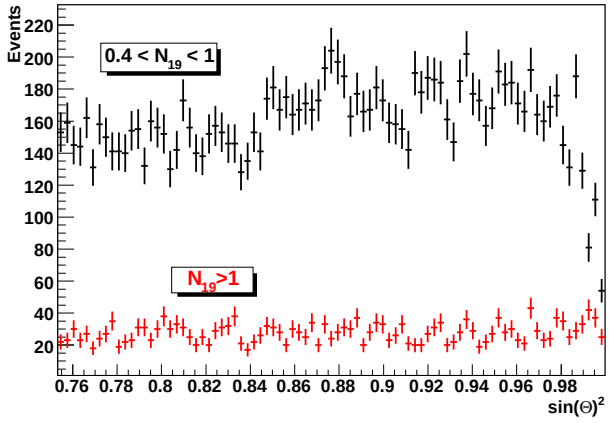

Fig. 2. Distribution of $\sin^2\theta$ for events which pass the T5 trigger and for $N_{19} > 1$ (lower red points) and $0.4 < N_{19} < 1$ (upper black points).

The shower core and the shower size are simultaneously estimated by a likelihood maximisation which accounts for non–triggering and saturated stations. The result of this maximisation procedure is then, the shower size parameter, which can be interpreted as the total number of muons in the shower. From Monte Carlo simulations, it has been found that the number of muons scales with the shower energy and independently of the zenith angle. For convenience, the maps have been normalised by the use of N_{19}. $N_{19} = 1$ means that the shower has the same number of muons as a proton shower generated with QGSJET and of energy 10^{19} eV.

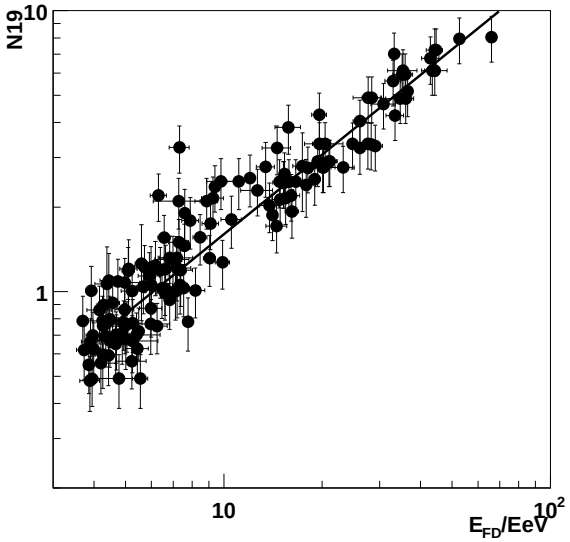

Fig. 3. The N_{19} parameter as a function of the FD energy in EeV. The line is the calibration fit with parameters $a = -0.72 \pm 0.03$ and $b = 0.94 \pm 0.03$, see the text.

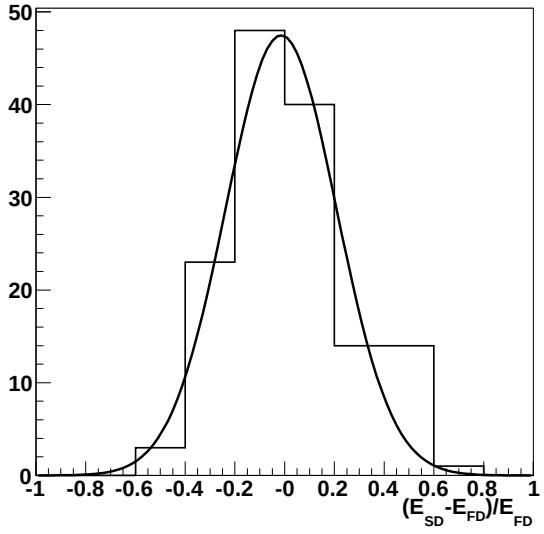

Fig. 4. Relative differences between the FD energy and the calibrated SD energy for events used in the calibration. The line is a Gaussian fit of average 0.01 $\pm$0.02 and RMS 0.22.

In this way, the zenith angle dependence of the shower size parameter is automatically taken into account. The uncertainty in the determination of N_{19} has been splitted in three terms:

$$\sigma^2_{N_{19}} = \sigma^2_{\rm stat} + \sigma^2_\theta + \sigma^2_{\rm sh}; \qquad (1)$$

where $\sigma_{\rm stat}$ is the statistical uncertainty, obtained from the maximum likelihood, σ_θ is the uncertainty in N_{19} due to the angular reconstruction uncertainty, and $\sigma_{\rm sh}$ is the uncertainty due to the shower–to–shower fluctuations in the number of muons. For the high energy showers considered in this work ($E > 6.3 \times 10^{18}$ eV), $\sigma_{\rm stat} < 10\%$, $\sigma_\theta < 6\%$ and the shower–to–shower fluctuations induce a fluctuation of the order of 18 % in N_{19}, making an overall uncertainty of the order of 22 %.

In figure 2, we show the distribution of $\sin^2(\theta)$ of events with $N_{19} > 1$ and $0.4 < N_{19} < 1$. It can be seen that the distribution for $N_{19} > 1$ is flat, showing that the array is fully efficient for $N_{19} > 1$ ($E > 6.3 \times 10^{18}$ eV).

In addition, systematic uncertainties in the determination of N_{19} have been estimated as follows. Several models of the reconstruction procedure are taken into account, including different muon map implementations (generated with Aires and CORSIKA) [1], [13], detector responses, and minimisation procedures. In the present work, two independent reconstruction codes (called A and B) have been used with different muons maps and tank responses. From this, a systematic uncertainty of the order of 20% is obtained for the N_{19}. Below, we will show that most of this uncertainty is reabsorbed in the process of calibration.

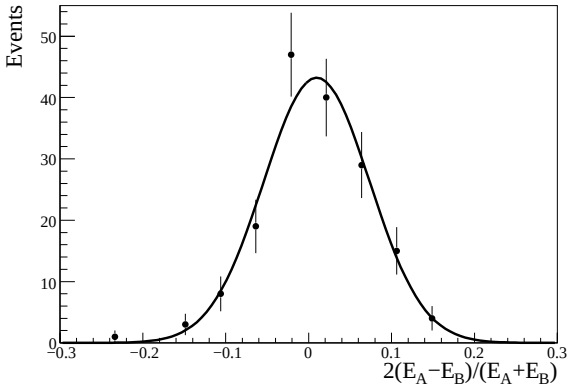

Fig. 5. Relative difference between the energy reconstructed with the two different SD reconstruction procedures A and B, as discussed in the text, for events above $E = 10^{19}$ eV. The line is a Gaussian fit to the histogram with reduced χ^2 5.9/10, mean 0.014 ± 0.006 and RMS 0.068 ± 0.005.

IV. CALIBRATION

The absolute energy scale is calibrated using the same procedure adopted in vertical showers, see [14]. A subsample of inclined hybrid events of good quality is selected using a set of cuts [12], optimised for inclined events. For inclined showers, no event above 75° survives the cuts. The energy reconstruction procedure used in the Fluorescence Detector has been described in [11]. Events reconstructed in the SD with $N_{19} < 0.4$ are not considered. This calibration procedure is done independently for the two reconstruction methods discussed earlier. For instance, for the code A, the correlation between the energy obtained from the FD reconstruction and N_{19} is shown in figure 3, where the

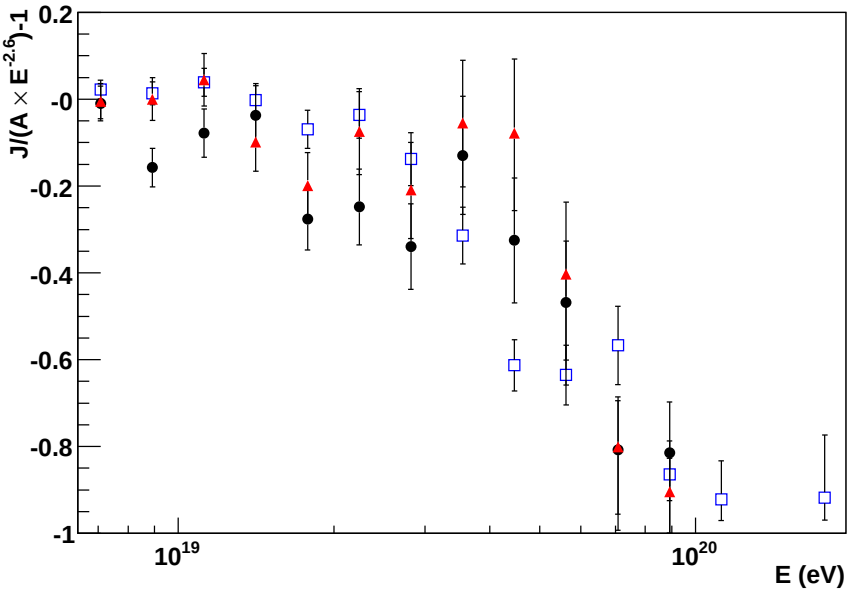

Fig. 6. Fractional differences ($J/(A\times E^{2.6})-1$) for the fluxes obtained with the two reconstruction procedures (A (circles) and B (triangles) for inclined events as a function of the energy. Also shown are the raw vertical data [10] (squares).

linear fit $\log_{10}(N_{19}^A) = a_A + b_A \log_{10}(E_{\rm FD})$ is also shown. The best fit yields the values $a_A = -0.72 \pm 0.03$ and $b_A = 0.94 \pm 0.03$. In figure 4, we show the relative difference between the energy reconstructed with the Fluorescence Detector and the Surface Detector for these events. A fractional RMS of 22% is found between the two reconstructions, compatible with the estimated uncertainty in the FD reconstruction and the SD reconstruction. The same procedure is applied to the reconstruction code B, obtaining a calibration curve with parameters $a_B = -0.6 \pm 0.01$ and $b_B = 0.93 \pm 0.02$. In the figure 5, we show the relative difference between the two reconstructed energies after the calibration for events above 10^{19} eV. The mean difference between the two reconstructed energies is below 2 % and the RMS is of the order of 7%. Therefore, the systematic uncertainty arising from the different reconstruction methods is absorbed in the calibration process, resulting in a systematic uncertainty of the order of 2 %. Other possible sources of systematics are currently under investigation.

V. Results and Discussion

Inclined events recorded from 1 January 2004 to 31 December 2008 were analysed using the procedures outlined above. It was found that above $E = 6.3$ EeV the array is fully efficient to T5HAS triggers (efficiency greater than 98 %). A total of 1750 events where selected above this energy. The fractional difference ($J/(A \times E^{-2.6}) - 1$, where A is a constant) is plotted in figure 6 for the two inclined spectra (A and B) and for the raw vertical spectrum supplied by the authors of [10]. At $\log_{10}(E/{\rm eV}) < 19.2$ differences between the two inclined spectra are of the order of 10 %. At higher energy, the difference can be as large as 30 %. A power–law fit to the spectra for inclined events gives a slope of $\gamma = 2.79 \pm 0.06$ in the energy range 6.3×10^{18} eV to 4.5×10^{19} eV. Above 4.5×10^{19} eV a power–law fit results in a slope of $\gamma = 5.1 \pm 0.9$. Alternatively, extrapolating the power–law fit with $\gamma = 2.79 \pm 0.06$, we would expect 54 events above 4.5×10^{19} eV, where only 39 are observed.

The comparison of the inclined event spectrum to the vertical spectrum can have implications for analysis of composition and of hadronic models. A change on composition or hadronic model would imply a different relation between N_{19} and E to the one used here. This could be seen as a change on the inclined spectrum with respect to the vertical spectrum. This is currently under investigation.

References

[1] M. Ave, R.A. Vázquez, and E. Zas, Astropart. Phys. 14 (2000) 91. M. Ave. et al., Phys. Rev. Lett. 85 (2000) 2244.
[2] J. Abraham et al., Nucl. Inst. and Methods, A523 (2004) 50.
[3] D. Newton et al., Proc. ICRC 30th, 2007.
[4] P. Facal San Luis et al., Proc. ICRC 30th, 2007.
[5] J. Abraham et al., Phys. Rev. Lett. **100** (2008) 211101.
[6] D. Allard et al., Proc. ICRC 29th, 2005.
[7] D. Allard et al., Proc. ICRC 29th, 2005.
[8] C. Bonifazi, et al., Proc. ICRC 29th, 2005.
[9] I. Valiño et al., these proceedings.
[10] F. Schüssler et al., these proceedings.
[11] B. Dawson et al., Proc. ICRC 30th, 2007.
[12] J. Abraham, et al., Phys. Rev. Lett. 101 (2008) 061101.
[13] H. Dembinski, P. Billoir, O. Deligny, and T. Hebbeker, arXiv:0904.2372.
[14] C. Di Giulio, et al., these proceedings.
[15] J. Tiffenberg et al., these proceedings.
[16] A. Castellina et al., these proceedings.